

¹ PeriDEM – High-fidelity modeling of granular media consisting of deformable complex-shaped particles

³ **Prashant Kumar Jha**  ¹

⁴ 1 Department of Mechanical Engineering, South Dakota School of Mines and Technology, Rapid City,
⁵ SD 57701, USA

DOI: [10.xxxxxx/draft](https://doi.org/10.xxxxxx/draft)

Software

- [Review](#) 
- [Repository](#) 
- [Archive](#) 

Editor: [Open Journals](#) 

Reviewers:

- [@openjournals](#)

Submitted: 01 January 1970

Published: unpublished

License

Authors of papers retain copyright and release the work under a Creative Commons Attribution 4.0 International License ([CC BY 4.0](#)).

⁶ Summary

⁷ Accurate simulation of granular materials under extreme mechanical conditions—such as crushing,
⁸ fracture, and large deformation—remains a significant challenge in geotechnical, manufacturing,
⁹ and mining applications. Classical discrete element method (DEM) models typically treat
¹⁰ particles as rigid or nearly rigid bodies, limiting their ability to capture internal deformation and
¹¹ fracture. The PeriDEM library, first introduced in ([Jha et al., 2021](#)), addresses this limitation
¹² by modeling particles as deformable solids using peridynamics, a nonlocal continuum theory
¹³ that naturally accommodates fracture and large deformation. Inter-particle contact is handled
¹⁴ using DEM-inspired local laws, enabling realistic interaction between complex-shaped particles.

¹⁵ Implemented in C++, PeriDEM is designed for extensibility and ease of deployment. It relies on
¹⁶ a minimal set of external libraries, supports multithreaded execution, and includes demonstration
¹⁷ examples involving compaction, fracture, and rotational dynamics. The framework facilitates
¹⁸ granular-scale simulations, supports the development of constitutive models, and serves as a
¹⁹ foundation for multi-fidelity coupling in real-world applications.

²⁰ Statement of Need

²¹ Granular materials play a central role in many engineered systems, but modeling their behavior
²² under high loading, deformation, and fragmentation remains an open problem. Popular open-
²³ source DEM codes such as YADE ([Smilauer et al., 2021](#)), BlazeDEM ([Govender et al., 2016](#)),
²⁴ Chrono DEM-Engine ([Zhang et al., 2024](#)), and LAMMPS ([Thompson et al., 2022](#)) are widely
²⁵ used but typically treat particles as rigid, limiting their accuracy in scenarios involving internal
²⁶ deformation and breakage. A recent review by Dosta et al. ([Dosta et al., 2024](#)) compares
²⁷ these libraries across a range of bulk processes. Meanwhile, peridynamics-based codes like
²⁸ Peridigm ([Littlewood et al., 2024](#)) and NLMech ([Jha & Diehl, 2021](#)) offer detailed fracture
²⁹ modeling but do not capture realistic particle contact mechanics or bulk granular dynamics.

³⁰ PeriDEM fills this gap by integrating state-based peridynamics for intra-particle deformation with
³¹ DEM-style contact laws for particle interactions. This hybrid approach enables direct simulation
³² of particle fragmentation, stress redistribution, and dynamic failure propagation—capabilities
³³ essential for modeling granular compaction, attrition, and crushing.

³⁴ Recent multiscale approaches, including DEM-continuum and DEM-level-set coupling methods
³⁵ ([Harmon et al., 2021](#)), attempt to bridge scales but often require homogenized assumptions.
³⁶ Sand crushing in geotechnical systems, for example, has been modeled using micro-CT-
³⁷ informed FEM or phenomenological laws ([Chen et al., 2023](#)). PeriDEM offers a particle-
³⁸ resolved alternative that allows bottom-up investigation of granular failure and shape evolution,
³⁹ especially in systems where fragment dynamics are critical.

⁴⁰ Background

⁴¹ The PeriDEM model was introduced in ([Jha et al., 2021](#)), demonstrating its ability to model
⁴² inter-particle contact and intra-particle fracture for complex-shaped particles. It is briefly
⁴³ described next.

⁴⁴ Brief Introduction to PeriDEM Model

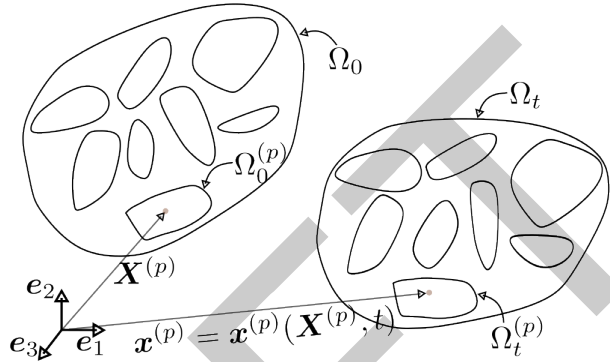


Figure 1: Motion of particle system.

⁴⁵ Consider a fixed frame of reference and $\{e_i\}_{i=1}^d$ are orthonormal bases. Consider a collection
⁴⁶ of N_P particles $\Omega_0^{(p)}$, $1 \leq p \leq N_P$, where $\Omega_0^{(p)} \subset \mathbb{R}^d$ with $d = 2, 3$ represents the initial
⁴⁷ configuration of particle p . Suppose $\Omega_0 \supset \cup_{p=1}^{N_P} \Omega_0^{(p)}$ is the domain containing all particles; see
⁴⁸ [Figure 1](#). The particles in Ω_0 are dynamically evolving due to external boundary conditions and
⁴⁹ internal interactions; let $\Omega_t^{(p)}$ denote the configuration of particle p at time $t \in (0, t_F]$, and
⁵⁰ $\Omega_t \supset \cup_{p=1}^{N_P} \Omega_t^{(p)}$ domain containing all particles at that time. The motion $x^{(p)} = x^{(p)}(\mathbf{X}^{(p)}, t)$
⁵¹ takes point $\mathbf{X}^{(p)} \in \Omega_0^{(p)}$ to $x^{(p)} \in \Omega_t^{(p)}$, and collectively, the motion is given by $\mathbf{x} = \mathbf{x}(\mathbf{X}, t) \in$
⁵² Ω_t for $\mathbf{X} \in \Omega_0$. We assume the media is dry and not influenced by factors other than
⁵³ mechanical loading (e.g., moisture and temperature are not considered). The configuration of
⁵⁴ particles in Ω_t at time t depends on various factors, such as material and geometrical properties,
⁵⁵ contact mechanism, and external loading. Essentially, there are two types of interactions
⁵⁶ present in the media:

- ⁵⁷ \blacksquare *Intra-particle interaction* that models the deformation and internal forces in the particle
⁵⁸ and
- ⁵⁹ \blacksquare *Inter-particle interaction* that accounts for the contact between particles and the boundary
⁶⁰ of the domain in which the particles are contained.

⁶¹ In DEM, the first interaction is ignored, assuming that particle deformation is insignificant
⁶² compared to inter-particle interactions. On the other hand, PeriDEM accounts for both
⁶³ interactions.

⁶⁴ The balance of linear momentum for particle p , $1 \leq p \leq N_P$, takes the form:

$$\rho^{(p)} \ddot{\mathbf{u}}^{(p)}(\mathbf{X}, t) = \mathbf{f}_{int}^{(p)}(\mathbf{X}, t) + \mathbf{f}_{ext}^{(p)}(\mathbf{X}, t), \quad \forall (\mathbf{X}, t) \in \Omega_0^{(p)} \times (0, t_F], \quad (1)$$

⁶⁵ where $\rho^{(p)}$, $\mathbf{f}_{int}^{(p)}$, and $\mathbf{f}_{ext}^{(p)}$ are density, and internal and external force densities. The
⁶⁶ above equation is complemented with initial conditions, $\mathbf{u}^{(p)}(\mathbf{X}, 0) = \mathbf{u}_0^{(p)}(\mathbf{X})$, $\dot{\mathbf{u}}^{(p)}(\mathbf{X}, 0) =$
⁶⁷ $\dot{\mathbf{u}}_0^{(p)}(\mathbf{X})$, $\mathbf{X} \in \Omega_0^{(p)}$.

68 **Internal force - State-based peridynamics**

69 The internal force term $f_{int}^{(p)}(\mathbf{X}, t)$ in the momentum balance governs intra-particle deformation
 70 and fracture. In PeriDEM, this term is modeled using a simplified state-based peridynamics for-
 71 mulation that accounts for nonlocal interactions over a finite horizon. The specific constitutive
 72 structure used—including damage-driven bond weakening, volumetric strain contributions, and
 73 neighbor-weighted quadrature—is discussed in detail in (Jha et al., 2021, sec. 2.1 and 2.3).
 74 This formulation allows unified simulation of deformation and fracture in individual particles.

75 **DEM-inspired contact forces**

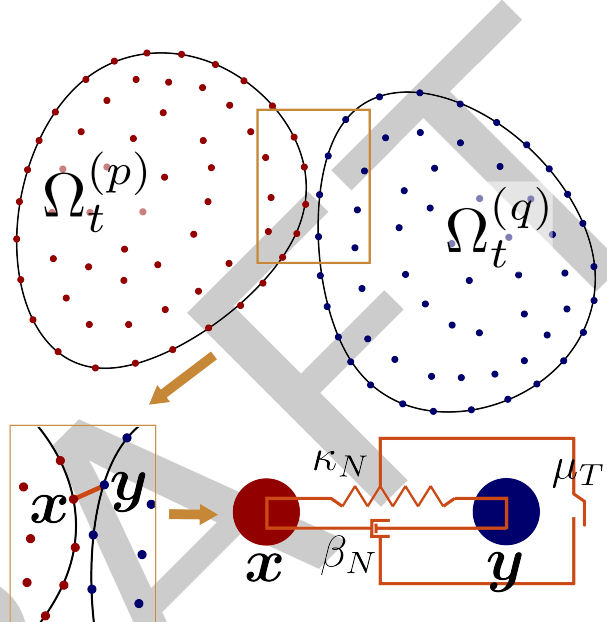


Figure 2: High-resolution contact approach in PeriDEM model for granular materials? between arbitrarily-shaped particles. The spring-dashpot-slider system shows the normal contact (spring), normal damping (dashpot), and tangential friction (slider) forces between points x and y .

76 The external force term $f_{ext}^{(p)}(\mathbf{X}, t)$ includes body forces, wall-particle interactions, and contact
 77 forces from other particles. Contact is modeled using a spring-dashpot-slider formulation applied
 78 locally when particles come within a critical distance. This approach introduces nonlinear normal
 79 forces, damping, and friction without relying on particle convexity or simplified geometries.
 80 Figure 2 illustrates the local high-resolution contact approach between deformable particles.
 81 The full formulation of contact detection, force assembly, and its implementation is provided
 82 in (Jha et al., 2021, sec. 2.2).

83 **Implementation**

84 PeriDEM is implemented in C++ and hosted on GitHub. It is designed for rapid deployment
 85 and extensibility, using a minimal set of external libraries bundled in the external directory. The
 86 core simulation model is implemented in `src/model/dem`, with the class `DEMModel` managing
 87 particle states, force calculations, and time integration.
 88 The code uses:
 89 - Taskflow (Huang et al., 2021) for multithreaded parallelism
 90 - nanoflann (Blanco & Rai, 2014) for efficient neighborhood search
 91 - VTK for output and post-processing
 92 The numerical strategies for neighbor search, peridynamic integration, damage evaluation,

92 and time stepping follow those introduced in (Jha et al., 2021, sec. 3), where additional
 93 implementation details and validation are discussed.

94 This work builds on earlier research in the analysis and numerical methods for peridynamics;
 95 see (Jha & Lipton, 2018a, 2018b, 2019; Jha & Lipton, 2020; Lipton et al., 2019).

96 Features

- 97 ▪ Hybrid modeling using peridynamics and DEM for intra-particle and inter-particle
 98 interactions
- 99 ▪ Simulation of deformation and breakage of a single particle under complex boundary
 100 conditions
- 102 ▪ Support for arbitrarily shaped particles, allowing for realistic simulation scenarios
- 104 ▪ Ongoing integration of MPI for distributed computing
- 106 ▪ Planned development of adaptive modeling strategies to enhance efficiency without
 107 compromising accuracy

109 Examples

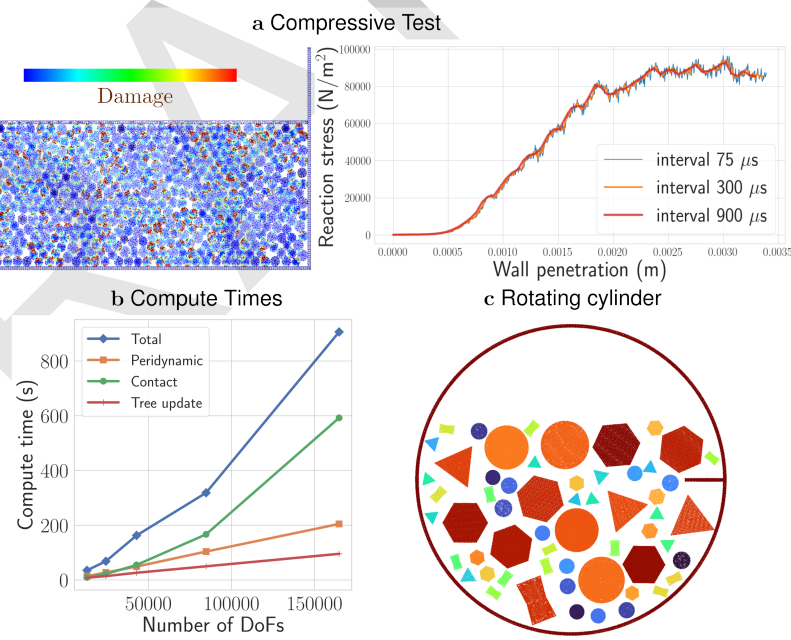


Figure 3: (a) Nonlinear response under compression, (b) exponential growth of compute time due to nonlocality of internal and contact forces, and (c) rotating cylinder with nonspherical particles.

110 Examples are described in [examples/README.md](#). One key case demonstrates compression
 111 of 500+ circular and hexagonal particles in a rectangular container by moving the top wall.
 112 The stress on the wall as a function of penetration becomes increasingly nonlinear as damage
 113 accumulates and the medium yields; see Figure 3a.

114 Preliminary performance tests show an exponential increase in compute time with the number
 115 of particles due to the nonlocal nature of both peridynamic and contact forces—highlighting
 116 a computational bottleneck. This motivates the integration of MPI and development of a

¹¹⁷ multi-fidelity framework. Additional examples include attrition of non-circular particles in a
¹¹⁸ rotating cylinder (Figure 3c).

¹¹⁹ References

- ¹²⁰ Blanco, J. L., & Rai, P. K. (2014). *Nanoflann: A C++ header-only fork of FLANN, a library*
¹²¹ *for nearest neighbor (NN) with KD-trees.* <https://github.com/jlblancoc/nanoflann>.
- ¹²² Chen, Q., Li, Z., Dai, Z., Wang, X., Zhang, C., & Zhang, X. (2023). Mechanical behavior and
¹²³ particle crushing of irregular granular material under high pressure using discrete element
¹²⁴ method. *Scientific Reports*, 13(1), 7843.
- ¹²⁵ Dosta, M., André, D., Angelidakis, V., Caulk, R. A., Celigueta, M. A., Chareyre, B., Dietiker, J.-
¹²⁶ F., Girardot, J., Govender, N., Hubert, C., & others. (2024). Comparing open-source DEM
¹²⁷ frameworks for simulations of common bulk processes. *Computer Physics Communications*,
¹²⁸ 296, 109066.
- ¹²⁹ Govender, N., Wilke, D. N., & Kok, S. (2016). Blaze-DEMGPU: Modular high performance
¹³⁰ DEM framework for the GPU architecture. *SoftwareX*, 5, 62–66.
- ¹³¹ Harmon, J. M., Karapiperis, K., Li, L., Moreland, S., & Andrade, J. E. (2021). Modeling
¹³² connected granular media: Particle bonding within the level set discrete element method.
¹³³ *Computer Methods in Applied Mechanics and Engineering*, 373, 113486.
- ¹³⁴ Huang, T.-W., Lin, D.-L., Lin, C.-X., & Lin, Y. (2021). Taskflow: A lightweight parallel and
¹³⁵ heterogeneous task graph computing system. *IEEE Transactions on Parallel and Distributed*
¹³⁶ *Systems*, 33(6), 1303–1320. <https://doi.org/10.1109/TPDS.2021.3104255>
- ¹³⁷ Jha, P. K., Desai, P. S., Bhattacharya, D., & Lipton, R. (2021). Peridynamics-based discrete
¹³⁸ element method (PeriDEM) model of granular systems involving breakage of arbitrarily
¹³⁹ shaped particles. *Journal of the Mechanics and Physics of Solids*, 151, 104376. <https://doi.org/10.1016/j.jmps.2021.104376>
- ¹⁴¹ Jha, P. K., & Diehl, P. (2021). NLMech: Implementation of finite difference/meshfree
¹⁴² discretization of nonlocal fracture models. *Journal of Open Source Software*, 6(65), 3020.
¹⁴³ <https://doi.org/10.21105/joss.03020>
- ¹⁴⁴ Jha, P. K., & Lipton, R. (2018a). Numerical analysis of nonlocal fracture models in holder
¹⁴⁵ space. *SIAM Journal on Numerical Analysis*, 56(2), 906–941. <https://doi.org/10.1137/17M1112236>
- ¹⁴⁷ Jha, P. K., & Lipton, R. (2018b). Numerical convergence of nonlinear nonlocal continuum
¹⁴⁸ models to local elastodynamics. *International Journal for Numerical Methods in Engineering*,
¹⁴⁹ 114(13), 1389–1410. <https://doi.org/10.1002/nme.5791>
- ¹⁵⁰ Jha, P. K., & Lipton, R. (2019). Numerical convergence of finite difference approximations for
¹⁵¹ state based peridynamic fracture models. *Computer Methods in Applied Mechanics and*
¹⁵² *Engineering*, 351, 184–225. <https://doi.org/10.1016/j.cma.2019.03.024>
- ¹⁵³ Jha, P. K., & Lipton, R. P. (2020). Kinetic relations and local energy balance for LEFM from
¹⁵⁴ a nonlocal peridynamic model. *International Journal of Fracture*. <https://doi.org/10.1007/s10704-020-00480-0>
- ¹⁵⁶ Lipton, R. P., Lehoucq, R. B., & Jha, P. K. (2019). Complex fracture nucleation and evolution
¹⁵⁷ with nonlocal elastodynamics. *Journal of Peridynamics and Nonlocal Modeling*, 1(2),
¹⁵⁸ 122–130. <https://doi.org/10.1007/s42102-019-00010-0>
- ¹⁵⁹ Littlewood, D. J., Parks, M. L., Foster, J. T., Mitchell, J. A., & Diehl, P. (2024). The
¹⁶⁰ peridigm meshfree peridynamics code. *Journal of Peridynamics and Nonlocal Modeling*,
¹⁶¹ 6(1), 118–148.

- 162 Smilauer, V., Angelidakis, V., Catalano, E., Caulk, R., Chareyre, B., Chèvremont, W., Doro-
163 feenko, S., Duriez, J., Dyck, N., Elias, J., Er, B., Eulitz, A., Gladky, A., Guo, N., Jakob, C.,
164 Kneib, F., Kozicki, J., Marzougui, D., Maurin, R., ... Yuan, C. (2021). Yade documentation
165 (3rd edition). *Zenodo*. <https://doi.org/10.5281/zenodo.5705394>
- 166 Thompson, A. P., Aktulga, H. M., Berger, R., Bolintineanu, D. S., Brown, W. M., Crozier, P.
167 S., in 't Veld, P. J., Kohlmeyer, A., Moore, S. G., Nguyen, T. D., Shan, R., Stevens, M. J.,
168 Tranchida, J., Trott, C., & Plimpton, S. J. (2022). LAMMPS - a flexible simulation tool for
169 particle-based materials modeling at the atomic, meso, and continuum scales. *Computer
170 Physics Communications*, 271, 108171. <https://doi.org/10.1016/j.cpc.2021.108171>
- 171
- 172 Zhang, R., Tagliafierro, B., Vanden Heuvel, C., Sabarwal, S., Bakke, L., Yue, Y., Wei, X.,
173 Serban, R., & Negrut, D. (2024). Chrono DEM-Engine: A discrete element method
174 dual-GPU simulator with customizable contact forces and element shape. *Computer
175 Physics Communications*, 300, 109196. <https://doi.org/10.1016/j.cpc.2024.109196>
- 176

DRAFT